

30. OXYGEN-ISOTOPE COMPOSITION OF CHERT FROM THE MID-PACIFIC MOUNTAINS AND HESS RISE, DEEP SEA DRILLING PROJECT LEG 62¹

James R. Hein, U.S. Geological Survey, 345 Middlefield Road, Menlo Park, California
and
Hsueh-Wen Yeh, Hawaii Institute of Geophysics, University of Hawaii, Honolulu, Hawaii

ABSTRACT

We measured oxygen-isotope compositions of 16 siliceous rocks from Deep Sea Drilling Project Sites 463, 464, 465, and 466 (Leg 62). Samples are from deposits that range in age from about 40 to 103 m.y. and that occur at sub-bottom depths of 9 to 461 meters. Mean $\delta^{18}\text{O}$ values range from 28.4 to 36.8‰ and $36.0 \pm 0.3\%$ for quartz-rich and opal-CT-rich rocks, respectively. $\delta^{18}\text{O}$ values in chert decrease with increasing sub-bottom depth; the slope of the $\delta^{18}\text{O}$ /depth curve is less steep for Site 464 than for the other sites which indicates that chert at Site 464 formed at higher temperatures than chert at Sites 463, 465, and 466. Temperatures of formation of cherts were 7 to 42°C, using the silica-water fractionation factor of Knauth and Epstein (1976), or 19 to 56°C, using the equation of Clayton et al. (1972). Temperatures in the sediment where the cherts now occur are lower than their isotopically determined temperatures of formation, which means that the cherts record an earlier history when temperatures in the sediment section were greater. Estimated sediment temperatures when the cherts formed are comparable to, but generally slightly lower than, those calculated from Knauth and Epstein's equation. The isotopic composition of cherts is more closely related to environment of formation (diagenetic environment) or paleogeothermal gradients, than to paleoclimates (bottom-water temperatures). Opal-CT-rich rocks may better record paleo-bottom-water temperature.

In Leg 62 cherts, better crystallinity of quartz corresponds to lower $\delta^{18}\text{O}$ values; this implies progressively higher temperatures of equilibration between quartz and water during maturation of quartz. The interrelationship of $\delta^{18}\text{O}$ and crystallinity is noted also in continental-margin deposits such as the Monterey Formation—but for higher temperatures. The apparent temperature difference between open-ocean and continental-margin deposits can be explained by the dominant control of temperature on silica transformation in the rapidly deposited continental-margin deposits, whereas time, as well as temperature, has a strong influence on the transformations in open-ocean deposits.

Comparisons between the chemistry and $\delta^{18}\text{O}$ values of cherts reveal two apparent trends: both boron and SiO_2 increase as $\delta^{18}\text{O}$ increases. However, the correspondence between SiO_2 and $\delta^{18}\text{O}$ is only apparent, because the two cherts lowest in SiO_2 are also the most deeply buried, so the trend actually reflects depth of burial. The correspondence between boron and $\delta^{18}\text{O}$ supports the conclusion that boron is incorporated in the quartz crystal structure during precipitation.

INTRODUCTION

We determined the oxygen-isotope compositions of 16 siliceous rocks cored during DSDP Leg 62 (Fig. 1). The analyzed rocks include 13 cherts and jaspers, one siliceous chalk, one quartz porcellanite, and one porcellanite containing quartz and opal-CT (Table 1). We discuss the isotopic compositions in relation to temperatures of formation and the chemical and mineralogical compositions of the cherts. Temperatures of formation were determined both with the empirically derived fractionation factor of Knauth and Epstein (1976), and with the experimentally derived SiO_2 -water fractionation factor of Clayton et al. (1972). The 16 siliceous rocks discussed here are a subset of the 65 siliceous rocks described by Hein et al. (this volume), who give detailed descriptions and chemical analyses of the rocks.

Samples analyzed for their oxygen-isotope compositions are from chalk and limestone at Sites 463, 465, and 466 and from pelagic clay and marlstone at Site 464. The distributions of the analyzed siliceous rocks with respect to lithologies and time are displayed in Figure 2. At Site 463, 822.5 meters of Quaternary through upper

Barremian nannofossil ooze, chalk, and limestone with minor amounts of chert and volcanic ash were drilled. At Site 464, 308.5 meters of Quaternary to Upper Miocene siliceous clay, lower Miocene to Upper Cretaceous brown clay, Cenomanian to upper Aptian chert and nannofossil limestone, and highly altered tholeiitic basalt were drilled. At Site 465 (Holes 465 and 465A), on Southern Hess Rise, 476 meters of Quaternary through upper Albian calcareous ooze, limestone, minor chert, and highly altered trachyte were drilled. At Site 466, also on southern Hess Rise, 312 meters of Quaternary to upper Albian calcareous sediments with minor chert and pyritic clay were drilled.

METHODS

The fluorination method of Taylor and Epstein (1962) was used to extract oxygen from the siliceous rocks for determination of $^{18}\text{O}/^{16}\text{O}$ ratios. Samples were quantitatively converted to CO_2 and isotopically analyzed with a dual-collector mass spectrometer. Results are reported as $\delta^{18}\text{O}_{\text{SMOW}}$ values that are the per mill deviation of the $^{18}\text{O}/^{16}\text{O}$ ratio of a sample from that of standard mean ocean water (SMOW) (Craig, 1961). Two (and in one case three) extractions and $^{18}\text{O}/^{16}\text{O}$ determinations were made on each sample. The mean $\delta^{18}\text{O}_{\text{SMOW}}$ values, replicate run values, and the deviations from means are reported in Table 1.

Siliceous rocks were pretreated before isotopic analysis: (1) carbonate minerals were removed with dilute 10% HCl (by volume); the

¹ Initial Reports of the Deep Sea Drilling Project, Volume 62.

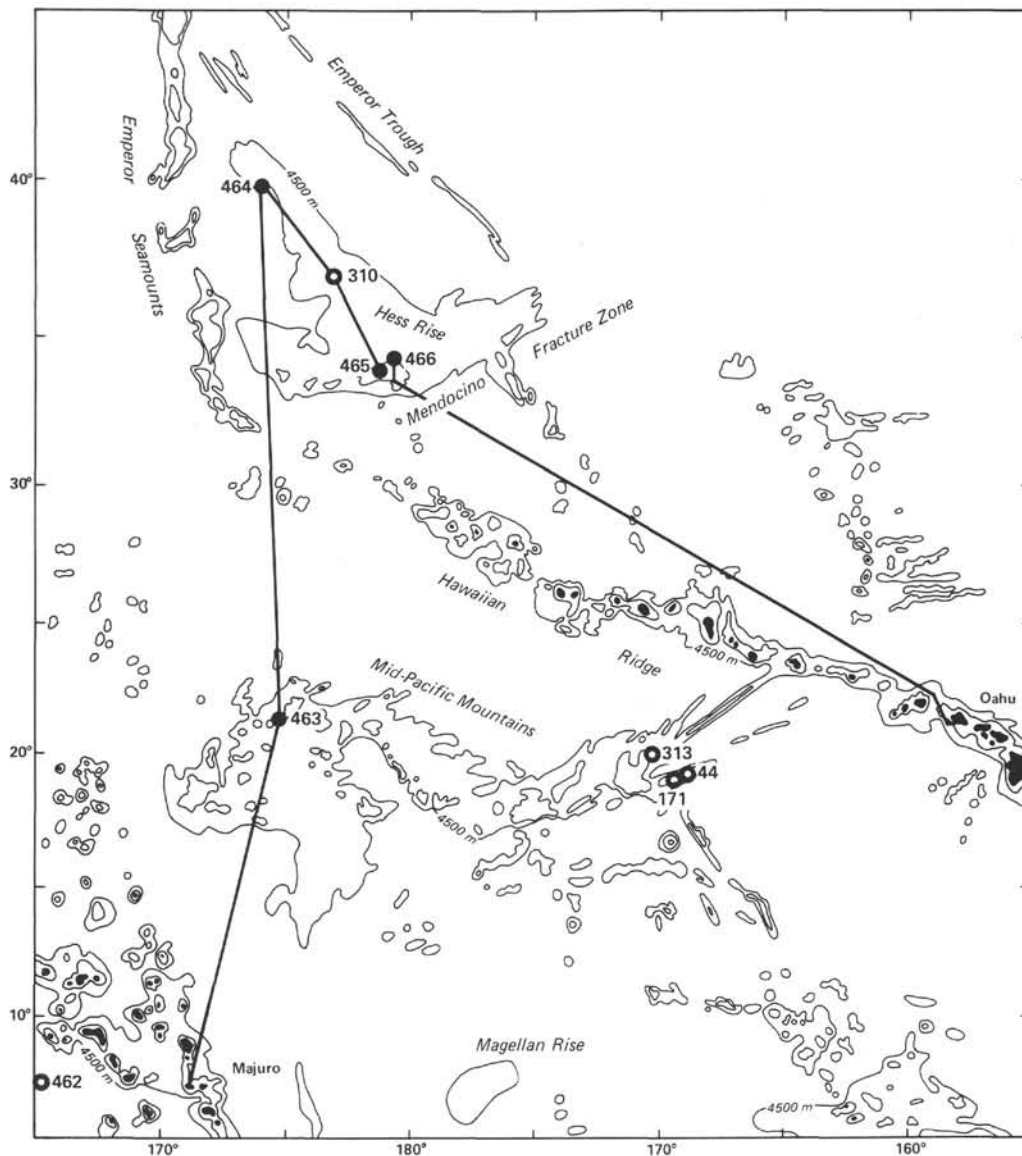


Figure 1. Location of Sites 463, 464, 465, and 466 (Leg 62), and other DSDP Sites. Solid circles are locations of measurements of thermal conductivities and heat flows used in Table 2 (Jessop et al., 1976).

treatment was carried out at room temperature and has no effect on the $\delta^{18}\text{O}_{\text{SMOW}}$ of the chert (Yeh and Epstein, in prep.); (2) the absorbed and other loosely bound waters were removed from the chert prior to fluorination, by heating the samples at about 250°C under high vacuum. After dehydration, samples were loaded into Ni reaction vessels under zero-humidity atmosphere.

Coexisting opal-CT and quartz were not separated before isotopic analysis. Values of $\delta^{18}\text{O}$ for these samples (Table 1) are probably higher than they would be if the quartz were isolated and analyzed separately, if Knauth and Epstein's (1975) and Pisciotto's (1978) observations are applicable to our samples. Major, minor, and trace elements of the cherts analyzed for their oxygen-isotope compositions are presented by Hein et al. (this volume).

ANALYTICAL RESULTS

Analyzed cherts are from deposits that range in age from about 40 to 103 m.y. and that occur at sub-bottom depths of 9 to 461 meters. Mean $\delta^{18}\text{O}$ values range from

28.4 to 36.8‰ for quartz-rich samples, and 36.0 and 36.3‰ for the two opal-CT-rich rocks. These values fall within the range of 27.1 to 41.8‰ reported for other marine cherts and porcellanites (Knauth and Epstein, 1975; Levitan et al., 1975; Kolodny and Epstein, 1976; Kastner, 1976). The average of mean $\delta^{18}\text{O}$ values and maximum and minimum $\delta^{18}\text{O}$ values become progressively higher from Site 464, on northern Hess Rise, to Site 463, in the Mid-Pacific Mountains, to Sites 465 and 466, on southern Hess Rise.

$\delta^{18}\text{O}$ values of cherts show well-defined decreases with increasing depth of occurrence at Sites 463, 464, and 465, if values for opal-CT-rich rocks are excluded (Fig. 3). We are not sure why $\delta^{18}\text{O}$ values for Site 466 cherts do not define a straight line (Fig. 3), but two possibilities are: (1) if Sample 466-9-1, 64 cm contains much organic C, analytical precision would be poor; or (2) if

Table 1. $\delta^{18}\text{O}_{\text{SMOW}}$ values of DSDP Leg 62 cherts.

Sample	Lithology	Mineralogy				$\delta^{18}\text{O}_{\text{SMOW}}$ (replicate runs)	$\delta^{18}\text{O}_{\text{SMOW}}$ (mean)	Deviation from the Mean
		Major	Moderate	Minor	Trace			
463-6-6, 36 cm	Tan chert	Quartz		Calcite		35.5 36.0	35.8	0.25
463-10-6, 82 cm	Siliceous chalk	Calcite	Opal-CT	Quartz	Smectite	35.7 36.2	36.0	0.25
463-22,CC (A)	Brown chert	Quartz			Smectite	32.7 33.4	33.1	0.35
463-52,CC	Calcareous gray chert	Quartz			Smectite	28.0 28.8	28.4	0.40
464-10-3, 70 cm	White chert	Calcite Quartz		Opal-CT		35.6 35.7	35.7	0.05
464-10-4, 34 cm (A)	Brown chert	Quartz			Smectite, calcite	33.8 34.1	34.0	0.15
464-11-1, 41 cm	Orange jasper	Quartz			Opal-CT	32.9 32.9	32.9	0.00
464-14-1, 40 cm	Black chert	Quartz			Smectite, Pyrite	33.1 33.2	33.2	0.05
464-17,CC	Red-brown jasper	Quartz		Calcite	Smectite	27.8 30.2 28.7	28.9	1.20
465-2,CC (A)	Gray transparent chert	Quartz				36.3 37.0	36.7	0.35
465-2,CC (B)	Quartz porcellanite	Quartz		Apatite		36.8 36.7	36.8	0.05
465A-40-1, 26 cm	Tuffaceous black chert	Quartz				29.9 30.1	30.0	0.10
466-9-1, 64 cm	Gray chert	Quartz		Barite	Gypsum, smectite	33.8 34.0	33.9	0.10
466-15-5, 45 cm	Brown jasper	Quartz		Barite	Smectite	34.9 35.7	35.3	0.40
466-27,CC (A)	Quartz, opal-CT, porcellanite	Opal-CT	Quartz		Barite	35.9 36.7	36.3	0.40
466-34-1, 8 cm (A)	Blue-gray chert	Quartz				32.8 33.0	32.9	0.10

Note: Calcite was removed from all samples before isotopic analysis.

the Pliocene–Eocene or Eocene–Maastrichtian unconformities at Site 466 (Fig. 2) are erosional rather than simply nondepositional, cherts from 466-9-1, 64 cm and 466-15-5, 45 cm could have formed at significantly different depths of burial than their present stratigraphic positions indicate. The $\delta^{18}\text{O}$ /depth curve for Site 464, on northern Hess Rise, has a markedly less steep slope than do the curves for the other sites.

$\delta^{18}\text{O}$ values of cherts show distinct variations with age of the enclosing sediment (Fig. 4). The few data available from Leg 62 samples show that $\delta^{18}\text{O}$ is increased about 3‰ for cherts in sediment deposited 80 to 90 m.y. ago, then is decreased 4‰ in sediment deposited back to about 115 m.y. ago, where $\delta^{18}\text{O}$ remains constant at about 33‰ back to 135 m.y. ago. Additional analyses may change this pattern significantly. Because chert does not form until 40 m.y. after deposition of the host sediment (Hein et al., this volume), the Cretaceous times just listed should be translated 40 m.y. toward the present to place the $\delta^{18}\text{O}$ changes into a more meaningful temporal scheme (see section on temperature of formation).

$\delta^{18}\text{O}$ and Silica Phases

No trend is evident in the $\delta^{18}\text{O}$ values of the three samples that contain more than a trace of opal-CT (Table 1). However, all three samples do fall within a narrow $\delta^{18}\text{O}$ range of $36.0 \pm 0.3\text{‰}$. In contrast, there is a parallel trend of $\delta^{18}\text{O}$ values and crystallinity of quartz (Fig. 5). Quartz crystallinity was measured according to the technique of Murata and Norman (1976) and is based on a scale of 10, plutonic quartz (high crystallinity) defining the high end, and diagenetic quartz (poor

crystallinity) defining the low end. For Leg 62 cherts, better crystallinity of quartz corresponds to lower $\delta^{18}\text{O}$ values, implying higher temperatures of equilibration between quartz and water during formation of better-crystallized quartz. The sample with the best crystallinity, 463-52,CC (Fig. 5), was also the most deeply buried (Table 2).

$\delta^{18}\text{O}$ and Chemical Composition of Chert

In general, the cherts are chemically very pure, averaging 96.17% SiO_2 ($\sigma = 0.92$) and 2.91% loss of fusion ($\sigma = 0.66$); that is, SiO_2 and volatiles exceed 99% (Hein et al., this volume). Of the cherts analyzed for their oxygen-isotope compositions, only that from 465A-40-1, 26 cm contains significant non-carbonate contamination (7.57% Al_2O_3). Comparisons between the chemistry (Hein et al., this volume) and the $\delta^{18}\text{O}$ values of cherts reveal two apparent trends: both SiO_2 and boron increase as $\delta^{18}\text{O}$ increases (Figs. 6 and 7). However, the correspondence of SiO_2 to $\delta^{18}\text{O}$ is only apparent, because the two cherts with the lowest SiO_2 concentrations (a calcareous and a tuffaceous chert; Table 1) are also the most deeply buried cherts (Fig. 6), so this trend actually reflects depth of burial. The trend between boron and $\delta^{18}\text{O}$ supports the conclusion that boron was incorporated in the quartz crystal structure during precipitation (Hein et al., this volume). No other trends are seen between $\delta^{18}\text{O}$ values and other elements analyzed. Especially noteworthy is the lack of correspondence between $\delta^{18}\text{O}$ and Al_2O_3 or CaO , suggesting that possible contamination by terrigenous, volcanic, and calcareous debris in the cherts has not significantly affected the isotopic values.

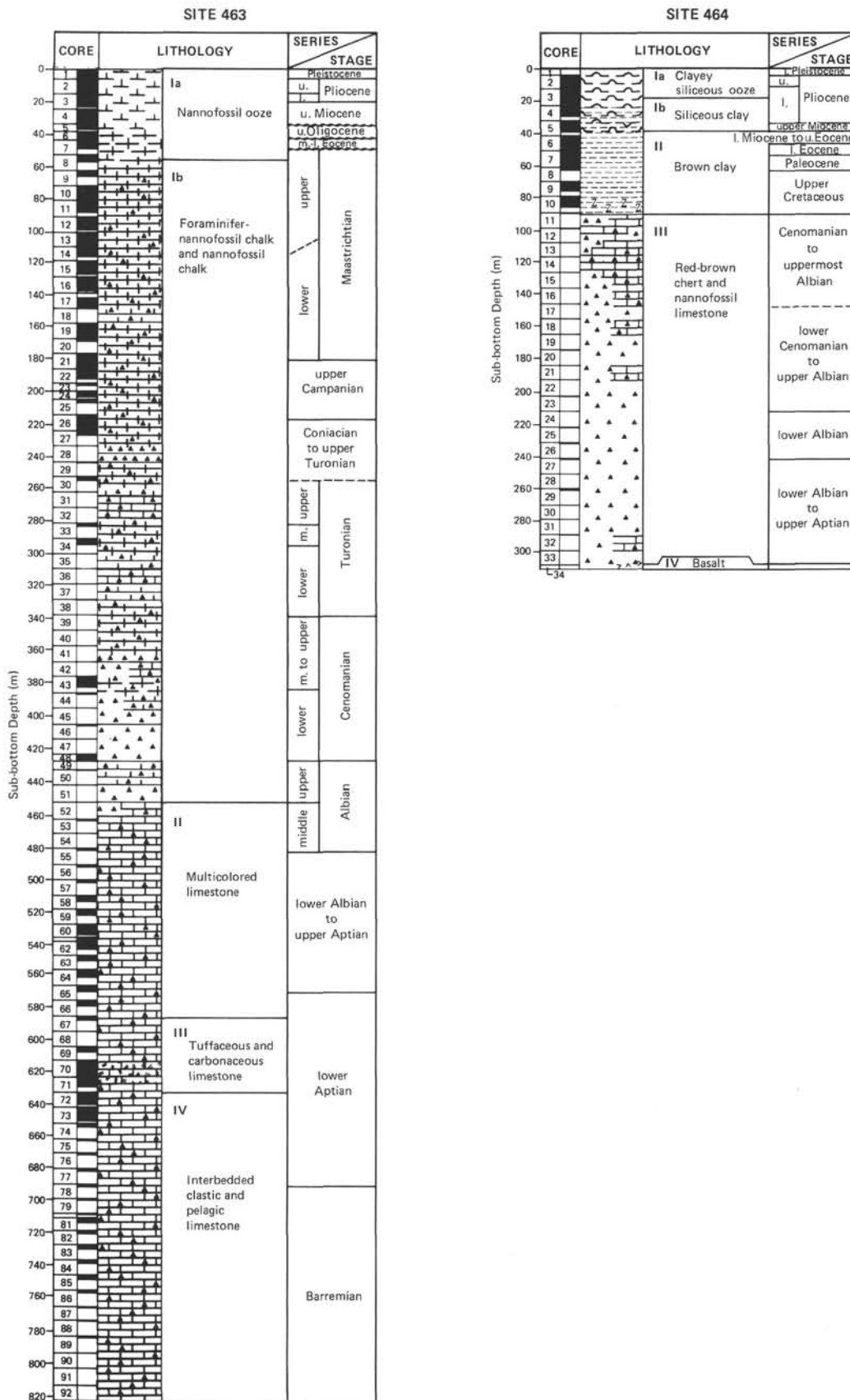


Figure 2. General lithologies, ages, and stratigraphic locations of cherts analyzed for oxygen-isotope compositions. See Tables 1 and 2 and Hein et al. (this volume) for descriptions of each studied rock.

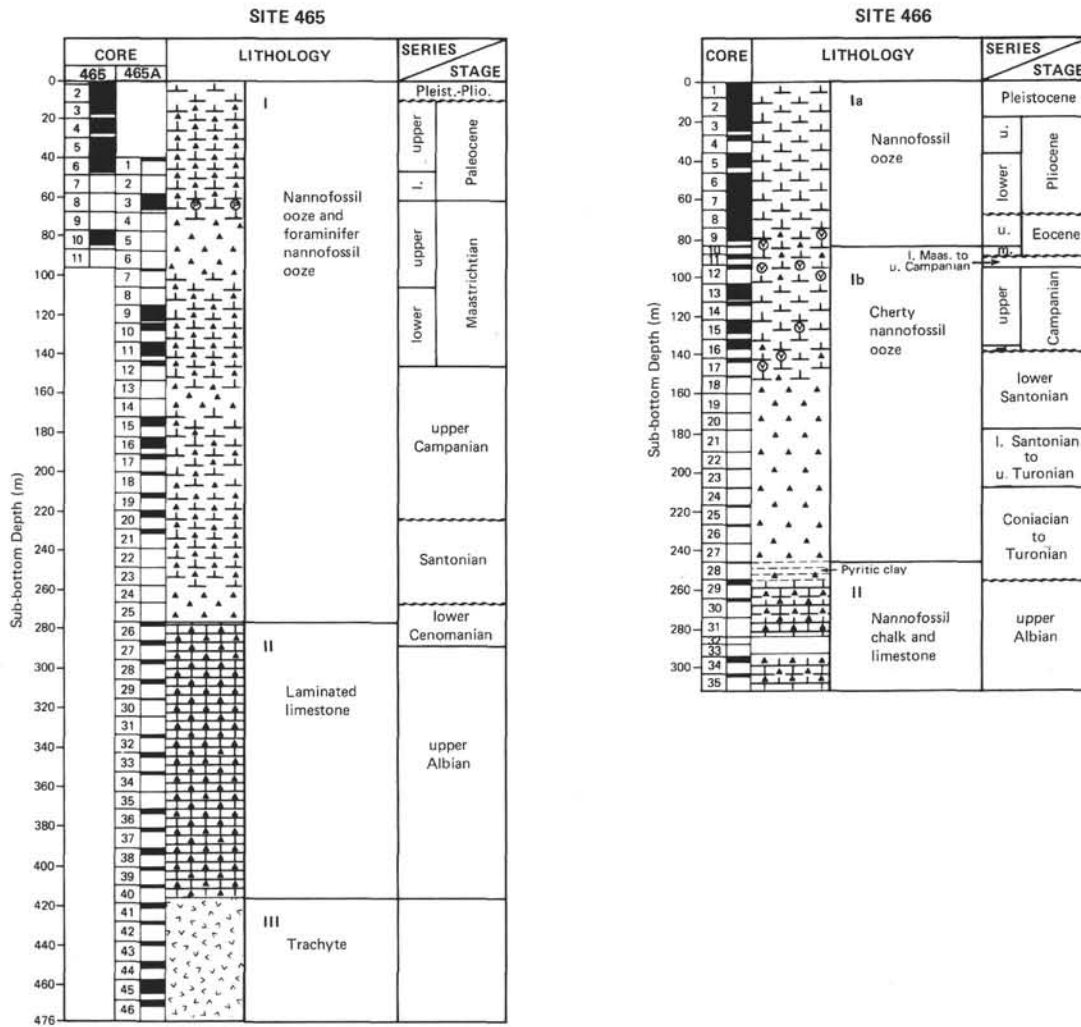


Figure 2. (Continued).

TEMPERATURE OF FORMATION

Temperatures of formation of cherts collected during Leg 62 were calculated from the equations of Knauth and Epstein (1976) and Clayton et al. (1972), assuming 0.0‰ for the waters of formation. The $\delta^{18}\text{O}$ value of pre-Pleistocene deep marine water has been suggested to be about -1.0‰ , which, if correct, would lower the isotopically derived temperatures by about 3°C (Table 2; Savin, 1977). Knauth and Epstein's quartz/water fractionation factor gives lower temperatures of formation ($7\text{--}42^\circ\text{C}$) than does that of Clayton et al. ($19\text{--}56^\circ\text{C}$) (Table 2; Fig. 8). The temperature in the sediment where the cherts were collected was calculated from estimated geothermal gradients for each site and from the depth of occurrence of each chert (Table 2); temperatures where the cherts occur now are lower than the temperatures of formation of the cherts determined from their oxygen-isotope compositions in all but one sample—that containing the most opal-CT. This means either that the cherts record an earlier history when temperatures in the sediments were greater, or that the oxygen-isotope

values of the waters of equilibration were significantly different from 0.0‰ .

We estimated the temperature of formation of each chert by assuming that most chert has formed by about 40 m.y. after the sediment in which it occurs was deposited (Hein et al., this volume), using the Cretaceous bottom-water temperatures of Douglas and Savin (1973), and assuming that Cretaceous geothermal gradients were similar to contemporary ones (Fig. 8). These assumptions produce temperatures of formation comparable with those calculated from Knauth and Epstein's (1976) equation (Fig. 8)—but on the average about 6°C lower (about 3.5°C if bottom-water had a $\delta^{18}\text{O}$ value of -1.0‰). Thus, data from Leg 62 cherts favor the validity of Knauth and Epstein's quartz/water fractionation factor for deep-sea cherts.

The greater the amount of opal-CT in a chert, the greater the degree of deviation from our curve of estimated temperature of formation (Fig. 8; points enclosed in rectangles). The sample with minor opal-CT falls on our curve, but those with intermediate to major amounts of opal-CT are displaced toward higher tem-

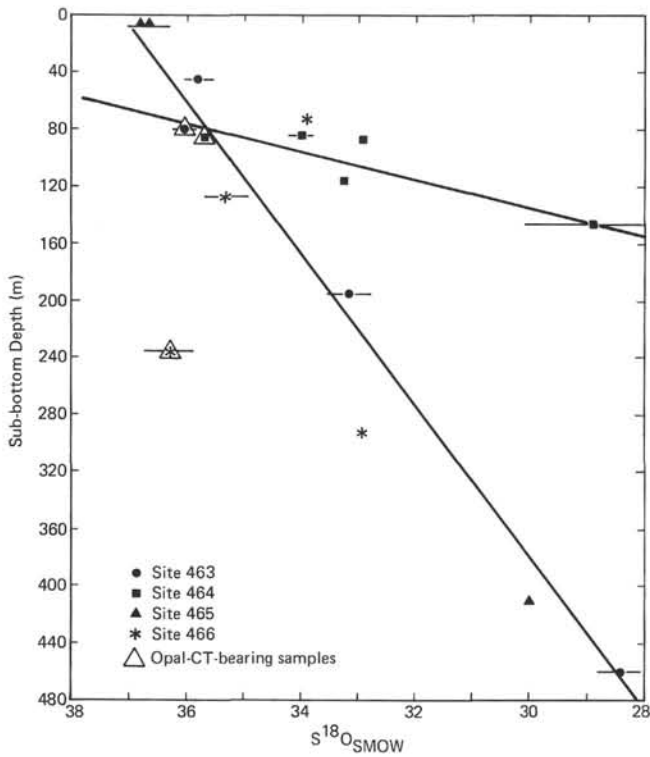


Figure 3. $\delta^{18}\text{O}$ compositions versus sub-bottom depths of Leg 62 cherts. Lines relate samples from the same sites.

temperatures of formation, one near the curve representing Knauth and Epstein's factor, and the other near the curve representing the factor of Clayton et al. The apparent higher temperatures of formation for opal-CT probably reflects the greater structural-water content in opal-CT; structural water would lower the $\delta^{18}\text{O}$ value for the bulk silica sample.

Two additional observations are apparent from Table 1 and Figure 8: (1) both chert and its quartz-porcellanite rim (465-2, CC) formed at the same temperature, in equilibrium with the same interstitial waters; this suggests either a simultaneous transformation from opal-CT to quartz within both the chert and porcellanite, or rapid quartz precipitation without an opal-CT precursor, the porcellanite reflecting a decrease in the availability of silica; (2) alteration of the trachytic basement rock at Site 465 did not change the isotopic composition of overlying interstitial waters enough to have a noticeable effect on the chert that formed in equilibrium with the interstitial water (see discussion by Lawrence et al., 1975).

DISCUSSION

Debate continues as to whether $\delta^{18}\text{O}$ values of marine cherts primarily reflect paleoclimates (bottom-water temperatures), or diagenetic environments (Degens and Epstein, 1962; Kolodny and Epstein, 1976; Knauth and Epstein, 1975). Kolodny and Epstein (1976) suggested

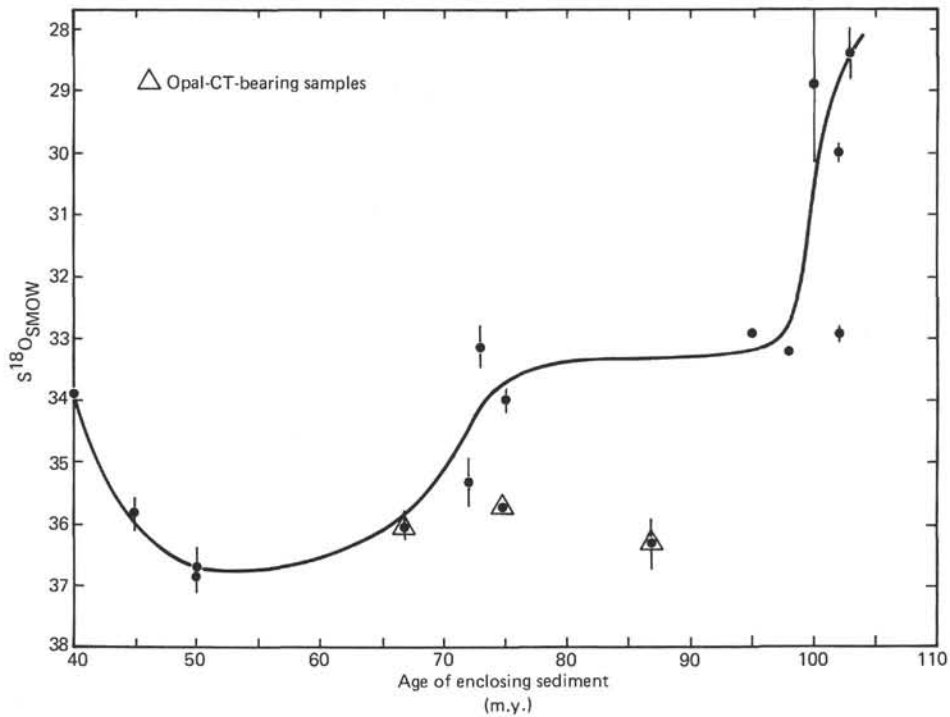


Figure 4. $\delta^{18}\text{O}$ compositions versus age of enclosing sediment of Leg 62 cherts. The triangle above 87 m.y. represents a sample composed mainly of opal-CT, which does not fit the trend of the other samples.

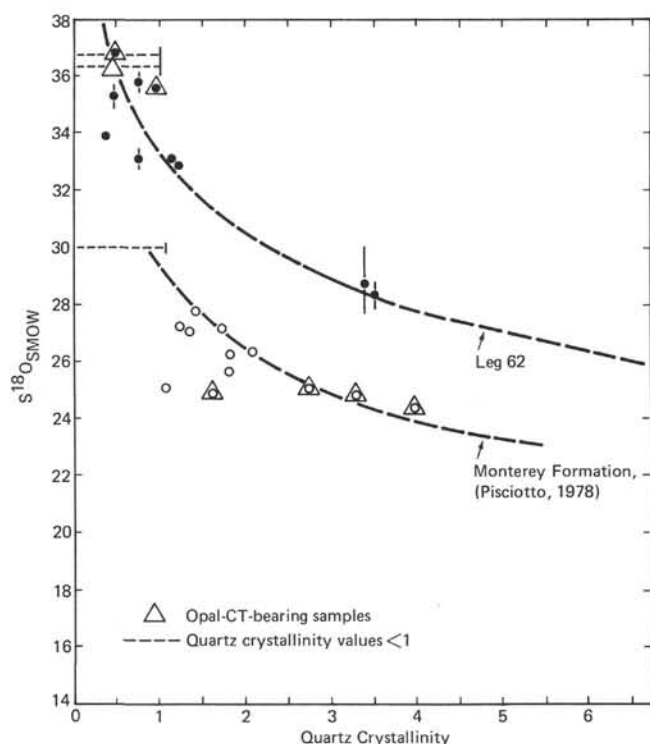


Figure 5. $\delta^{18}\text{O}$ compositions versus the crystallinity of quartz in Leg 62 cherts, and in chert and porcellanite from the Monterey Formation of California.

that the isotopic compositions of deep-sea cherts record paleo-bottom-water temperatures (our Fig. 9 shows Leg 62 data plotted on Kolodny and Epstein's fig. 5); they considered that a good match exists between their Tertiary-Cretaceous isotope-temperature curve and the bottom-water-temperature curve of Douglas and Savin (1973).

Data from Leg 62 cherts (ages translated 40 m.y. toward the present) describe a curve representing much greater paleotemperatures, but somewhat similar in the general trend of increasing temperatures with increasing age (Fig. 9); the temperature at which a chert formed depends on both bottom-water temperatures and the geothermal gradients, the higher the bottom-water temperature the greater should be its influence on the sub-bottom-sediment temperature at which the chert formed. Because Cretaceous bottom-water temperatures were much higher than Neogene temperatures, the Cretaceous temperatures derived from cherts should more closely approximate the Cretaceous bottom-water-temperature curve than do the temperatures determined from the Neogene samples, if in fact bottom-water temperature was the dominant control; the opposite effect is observed in Figure 9, suggesting that the isotopic compositions of Leg 62 cherts in large part record diagenetic environments or paleogeothermal gradients.

With the temperatures determined from the equations of Knauth and Epstein (1976), calculated paleo-

Table 2. Temperature and depth of formation of DSDP Leg 62 cherts.

Sample	Sub-bottom Depth of Cherts (m)	Age of Enclosing Sediment (m.y.)	Heat Flow ^a (HFU)	Thermal Conductivity ^b (mcal/cm-sec-°C)	Geothermal Gradient (°C/m)	$\delta^{18}\text{O}$ Temperature of Formation, ^c T_1 (°C)	$\delta^{18}\text{O}$ Temperature of Formation, ^d T_2 (°C)	Temperature Present at Depth of Bed (°C)	Calculated Temperature of Formation ^f (°C)
463-6-6, 36 cm	46	45	1.24	2.14	0.058	23	10	4	4
463-10-6, 82 cm	80	67	1.24	2.14	0.058	22	10	6	8
463-22, CC (A)	195	73	1.24	2.14	0.058	33	20	13	14
463-52, CC	461	103	1.24	2.14	0.058	56	42	28	37
Base of sediment section drilled	820	117	1.24	2.14	0.058	—	—	49	49
464-10-3, 70 cm	83	75	1.20	1.87/2.32	0.064/0.052	23	10	7/6	4/3
464-10-4, 34 cm (A)	84	75	1.20	1.87/2.32	0.064/0.052	31	18	7/6	4/3
464-11-1, 41 cm	89	95	1.20	1.87/2.32	0.064/0.052	34	21	7/6	15/14
464-14-1, 40 cm	118	98	1.20	1.87/2.32	0.064/0.052	33	20	9/8	17/16
464-17, CC	146	100	1.20	1.87/2.32	0.064/0.052	52	39	11/9	19/18
Base of sediment section drilled	310	115	1.20	1.87/2.32	0.064/0.052	—	—	21/17	29/26
465-2, CC (A)	9	50	1.36	3.32	0.041 ^g	20	8	2	5
465-2, CC (B)	9	50	1.36	3.32	0.041	19	7	2	5
465A-40-1, 26 cm	410	102	1.36	3.32	0.041	47	34	18	27
Base of sediment section drilled	415	104	1.36	3.32	0.041	—	—	19	27
466-9-1, 64 cm	75	40	1.36	3.32	0.041	30	17	4	4
466-15-5, 45 cm	128	72	1.36	3.32	0.041	25	12	7	7
466-27, CC (A)	236	87	1.36	3.32	0.041	21	9	11	18
466-34-1, 8 cm	293	102	1.36	3.32	0.041	34	21	13	19
Base of sediment section drilled	310	104	1.36	3.32	0.041	—	—	14	20

^a Site 463 based on average of 7 nearby heat-flow stations; Site 464 on 1 nearby station (see Fig. 1) from Jessop et al. (1976); Site 465 calculated from a geothermal gradient measured *in situ*; the Site 465 value is also used for Site 466.

^b Site 463 based on average of 8 nearby measurements from Jessop et al. (1976); Site 464 first value is average of 2 nearby measurements, second value is from shipboard measurements during Leg 62, as is the value for Site 465; the measured value at Site 465 is also used for Site 466.

^c Calculated from Clayton et al. (1972).

^d Calculated from Knauth and Epstein (1975).

^e Based on geothermal gradients in fourth column and bottom-water temperatures of 1.5°C.

^f 40 m.y. after deposition, using bottom paleotemperatures from Douglas and Savin (1973).

^g *In situ* measurement.

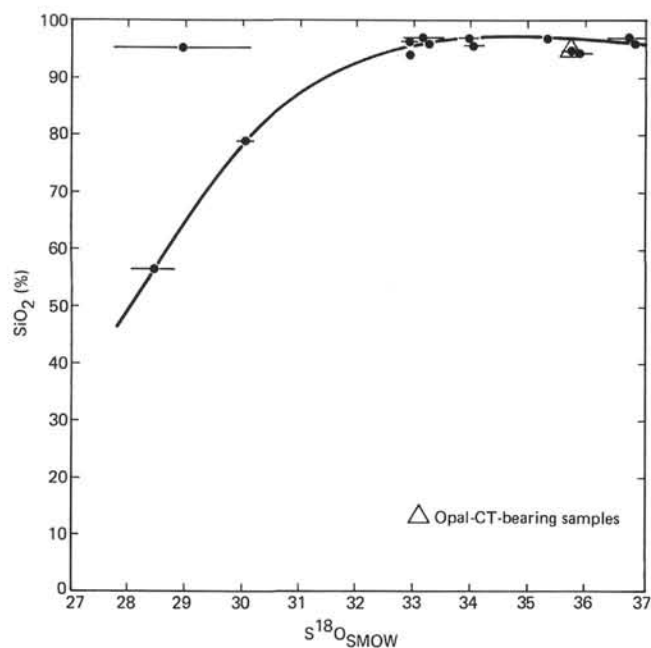


Figure 6. $\delta^{18}\text{O}$ versus SiO_2 content of Leg 62 cherts. Major and minor element compositions of Leg 62 cherts are presented by Hein et al. (this volume).

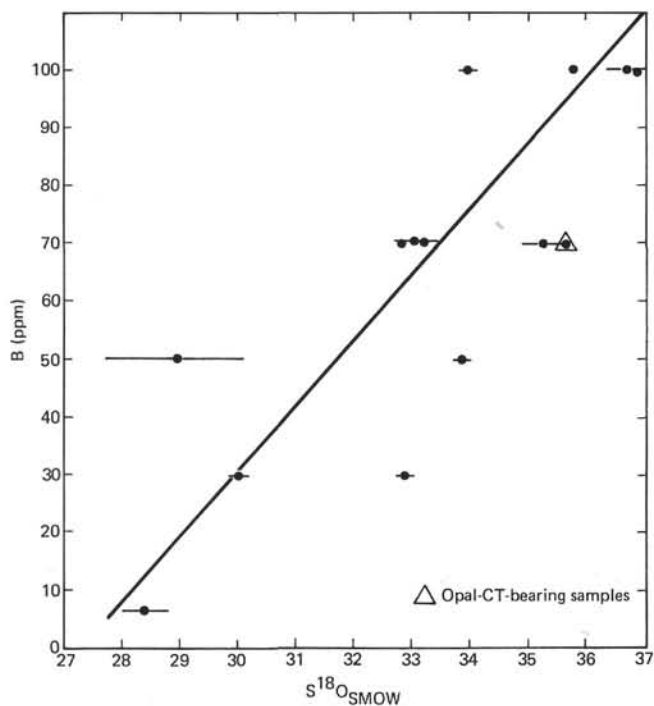


Figure 7. $\delta^{18}\text{O}$ versus boron contents of Leg 62 cherts.

geothermal gradients would be 0.08, 0.49, 0.06, and 0.05°C/m for Sites 463, 464, 465, and 466, respectively. Except for Site 464, these geothermal gradients are similar to, but slightly greater than, the contemporary gradients of 0.06, 0.06, 0.04, and 0.04°C/m for the same sites, respectively. We do not know why there is such a

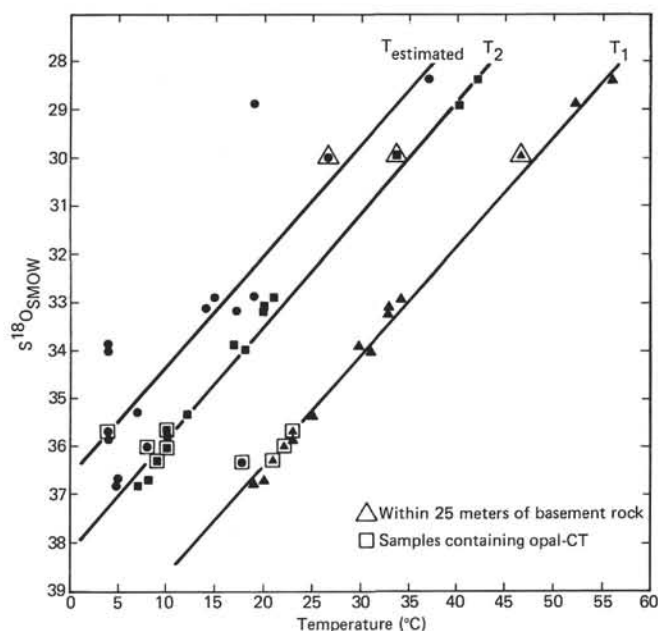


Figure 8. $\delta^{18}\text{O}$ compositions versus possible temperatures of formation of Leg 62 cherts. T_1 represents temperatures derived from the silica/water fractionation factor of Clayton et al. (1972). T_2 represents temperatures derived from the equation of Knauth and Epstein (1976). $T_{\text{estimated}}$ represents estimated temperatures of formation for cherts, assuming the various paleoceanographic conditions outlined in the text and in Table 2.

large discrepancy for Site 464; a possibility is that we may have incorrectly assumed a constant geothermal gradient for both the pelagic clay and the carbonate sections (Fig. 2). However, possible errors related to this assumption are probably not great enough to account for the large discrepancy between the paleogeothermal and contemporary geothermal gradients at Site 464. The location of Site 464 near the hot spot that created the adjacent Emperor Seamounts may have created a regime of higher temperatures at the site early in its history.

As suggested by Knauth and Epstein (1975), opal-CT-rich rocks may reflect bottom-water temperatures more than do quartz cherts. The one sample we analyzed that contains abundant opal-CT supports their notion, and plots much closer to the Douglas and Savin (1973) bottom-water-temperature curve than do other samples of the same age (Fig. 9). However, Knauth and Epstein caution that temperatures derived from opal-CT do not always agree with bottom-water temperatures obtained by other means.

COMPARISONS WITH CONTINENTAL-MARGIN SILICEOUS ROCKS

Hein et al. (1978) suggested that opal-A transforms into opal-CT faster and at higher temperatures in continental-margin deposits than in deep-sea, open-ocean deposits. Continental-margin deposits are characterized by high rates of sedimentation, and temperature is a dominant control in the transformation of silica, whereas in the open-ocean environment, where rates of

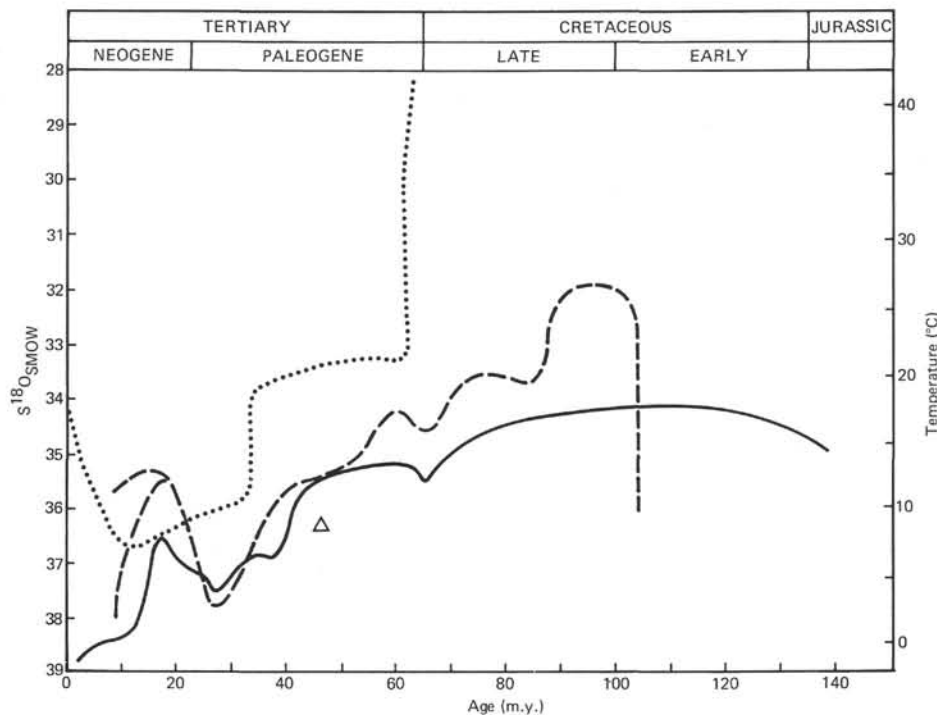


Figure 9. $\delta^{18}\text{O}$ and temperature, using Knauth and Epstein's (1976) curve, versus age. The curve derived from our data (dotted) and that from the data of Kolodny and Epstein (1976; dashed) are translated 40 m.y. toward the present, because deep-sea cherts take about 40 m.y. after deposition of the host sediment to form. The solid line represents Douglas and Savin's (1973) bottom-water temperature curve derived from isotopic analysis of benthic foraminifers. The triangle represents the Leg 62 sample composed mainly of opal-CT.

sedimentation are generally very low, time plays an increasingly important role relative to temperature (see fig. 9 of Hein et al., 1978; Pisciotto, 1978). In both environments, the chemistry of the host sediments and pore waters also influence silica transformations (Kastner et al. 1977; Knauth, 1979).

The transformation from opal-CT to quartz and the maturation of quartz in open-ocean cherts likewise may occur slower and at lower temperatures than the same transformations in continental-margin deposits. This relationship can be illustrated by comparing values of $\delta^{18}\text{O}$ versus quartz crystallinity of Leg 62 cherts with such values for siliceous rocks in the Monterey Formation of California (Fig. 5; Pisciotto, 1978); indeed, the curve for the Monterey Formation falls below (lighter $\delta^{18}\text{O}$, greater temperatures) that of Leg 62 cherts, suggesting higher temperatures of formation. An alternative explanation for the offset of the curves in Figure 5 is that Pisciotto (1978) may have assumed incorrectly a 0.0‰ value for the water in which the Monterey Formation siliceous deposits equilibrated.

ACKNOWLEDGMENTS

We appreciate technical and analytical help from Eva Vanek, Mary Ann Allan, Sara Monteith, and Dorothy Sicard, U.S. Geological Survey, and Crystal S. Lipton and Rita Pujale, University of Hawaii. L. Paul Knauth, Arizona State University, and George W. Moore and T. L. Vallier, U. S. Geological Survey, provided critical reviews. H.-W. Yeh acknowledges NSF Grant OCE-78-25283. Hawaii Institute of Geophysics contribution number 1048. Research completed in con-

junction with IGCP Project 115, Siliceous Deposits of the Pacific Region.

REFERENCES

- Clayton, R. N., O'Neil, J. R., and Mayeda, T. K., 1972. Oxygen isotope exchange between quartz and water. *J. Geophys. Res.*, 77: 3057-3067.
- Craig, H., 1961. Standards for reporting concentrations of deuterium and oxygen-18 in natural waters. *Science*, 133:1833-1834.
- Degens, E. T., and Epstein, S., 1962. Relation between $\text{O}^{18}/\text{O}^{16}$ ratios in coexisting carbonates, cherts, and diatomites. *Bull. Am. Assoc. Petrol. Geol.*, 46:534-542.
- Douglas, R. G., and Savin, S. M., 1973. Oxygen and carbon isotope analyses of Cretaceous and Tertiary foraminifera from the central North Pacific. In Winterer, E. L., Ewing, J. I., et al., *Init. Repts. DSDP*, 17: Washington (U.S. Govt. Printing Office), 591-605.
- Hein, J. R., Scholl, D. W., Barron, et al., 1978. Diagenesis of late Cenozoic diatomaceous deposits and formation of the bottom simulating reflector in the southern Bering Sea. *Sedimentology*, 25:155-181.
- Jessop, A. M., Hobart, M. A., and Sclater, J. G., 1976. The world heat flow data collection—1975. *Energy, Mines and Resources Canada, Earth Physics Branch, Geothermal Service of Canada*, 5.
- Kastner, M., 1976. Diagenesis of basal sediments and basalts of Sites 322 and 323, Leg 35, Bellinghousen Abyssal Plain. In Hollister, C. D., Craddock, C., et al., *Init. Repts. DSDP*, 35: Washington (U.S. Govt. Printing Office), 513-528.
- Kastner, M., Keene, J. B., and Gieskes, J. M., 1977. Diagenesis of siliceous oozes. I. Chemical controls on the rate of opal-A to opal-CT transformation—an experimental study. *Geochim. Cosmochim. Acta*, 41:1041-1059.
- Knauth, L. P., 1979. A model for the origin of chert in limestone. *Geology*, 7:274-277.

- Knauth, L. P., and Epstein, S., 1975. Hydrogen and oxygen isotope ratios in silica from the Deep Sea Drilling Project. *Earth Planet. Sci. Lett.*, 25:1-10.
- _____, 1976. Hydrogen and oxygen isotope ratios in modular and bedded cherts. *Geochim. Cosmochim. Acta*, 40:1095-1108.
- Kolodny, Y., and Epstein, S., 1976. Stable isotope geochemistry of deep sea cherts. *Geochim. Cosmochim. Acta*, 40:1195-1209.
- Lawrence, J. R., Gieskes, J. M., and Broecker, W. S., 1975. Oxygen isotope and cation composition of DSDP pore waters and the alteration of layer II basalts. *Earth Planet. Sci. Lett.*, 27:1-10.
- Levitan, M. A., Dontsova, E. I., Lisitsyn, A. P., et al., 1975. The origin of chert in the sediments of the Pacific Ocean from data of oxygen isotopic analysis and a study of the distribution of chert. *Geokhimiya*, 3:420-430.
- Murata, K. J., and Norman, M. B. II, 1976. An index of crystallinity for quartz. *Am. J. Sci.*, 276:1120-1130.
- Pisciotta, K. A., 1978. Basinal sedimentary facies and diagenetic aspects of the Monterey Shale, California [Ph.D. dissert.]. University of California, Santa Cruz.
- Savin, S. M., 1977. The history of the earth's surface temperature during the past 100 million years. *Ann. Rev. Earth Planet. Sci.*, 5:319-355.
- Taylor, H. P. Jr., and Epstein, S., 1962. Relationship between O^{18}/O^{16} ratios in coexisting minerals of igneous and metamorphic rocks: I. Principles and experimental results. *Geol. Soc. Am. Bull.*, 73:461-480.